Molecular Biology of the Cell
Vol. 18, 1645–1656, May 2007

Chromosome Malorientations after Meiosis II Arrest Cause Nondisjunction[V]

Marie A. Janicke,* Loren Lasko,* Rudolf Oldenbourg,† and James R. LaFountain, Jr.*

*Department of Biological Sciences, State University of New York at Buffalo, Amherst, NY 14260; and †Marine Biological Laboratory, Woods Hole, MA 02543

Submitted October 27, 2006; Revised January 16, 2007; Accepted February 9, 2007
Monitoring Editor: Kerry Bloom

This study investigated the basis of meiosis II nondisjunction. Cold arrest induced a fraction of meiosis II crane fly spermatocytes to form (n + 1) and (n − 1) daughters during recovery. Live-cell liquid crystal polarized light microscope imaging showed nondisjunction was caused by chromosome malorientation. Whereas amphitely (sister kinetochore fibers to opposite poles) is normal, cold recovery induced anaphase syntely (sister fibers to the same pole) and merotely (fibers to both poles from 1 kinetochore). Maloriented chromosomes had stable metaphase positions near the equator or between the equator and a pole. Syntelics were at the spindle periphery at metaphase; their sisters disconnected at anaphase and moved all the way to a centrosome, as their strongly birefringent kinetochore fibers shortened. The kinetochore fibers of merotelics shortened little if any during anaphase, making anaphase lag common. If one fiber of a merotelic was more birefringent than the other, the less birefringent fiber lengthened with anaphase spindle elongation, often permitting inclusion of merotelics in a daughter nucleus. Meroamphitely (near amphitely but with some merotely) caused sisters to move in opposite directions. In contrast, syntely and merosyntely (near syntely but with some merotely) resulted in nondisjunction. Anaphase malorientations were more frequent after longer arrests, with particularly long arrests required to induce syntely and merosyntely.

INTRODUCTION

Nondisjunction is the outcome of anomalous mitosis or meiosis in which one daughter nucleus gains an extra chromosome and the other daughter loses a chromosome. When nondisjunction occurs in meiosis, a resulting gamete having an extra chromosome can participate in fertilization to create an embryo with an extra chromosome. Such embryos suffer from serious disorders, Down's syndrome (trisomy 21) being a common example (Hassold and Hunt, 2001; Lamb and Hassold, 2004). Gametes with missing chromosomes produce embryos that are nonviable, except for sex chromosomes. Nondisjunction is one of two routes to aneuploidy (any change, be it a gain or a loss, in chromosome number other than complete multiples of the normal set). The other route to aneuploidy is chromosome loss from both daughter cells, generally attributed to chromosome lagging near the equator at anaphase (Ford *et al*., 1988). Somatic cell aneuploidy is associated with tumorigenesis and other disorders (Cimini and Degrassi, 2005; Kops *et al*., 2005).

The term nondisjunction may seem to imply a process in which partner chromosomes that should have segregated at anaphase failed to "disjoin" (Cimini *et al*., 1997) and thus moved, stuck together, to the same pole. Actually, nondisjunction often occurs because partners disconnect from one another prematurely (Lamb *et al*., 1996; Bickel *et al*., 1998; Rebollo and Arana, 1998). Normally, the back-to-back association of partner chromosomes helps them orient (attach via kinetochore fibers) to opposite poles, and this ensures that they segregate to opposite poles. In the absence of such pairing, orientation and hence the segregation it specifies, may be anomalous (Khodjakov *et al*., 1997; Nicklas, 1997; Yu and Dawe, 2000), leading to nondisjunction (Angell, 1997; Bickel *et al*., 1998; Hassold and Hunt, 2001; Tanaka, 2002; Kops *et al*., 2005).

Some of the few clear facts about nondisjunction are that 1) it is induced in mitotic or meiotic cells recovering from experimental spindle arrest (Hildreth and Ulrichs, 1969; Kato and Yosida, 1970; Tokunaga, 1970; Karp and Smith, 1975; Cimini *et al*., 1999); 2) it can occur naturally in mitosis (Cimini *et al*., 1999) or in the first meiotic division or the second meiotic division of either the male or female germline (Nicolaidis and Petersen, 1998), where it sometimes but not always correlates with premature disconnection of partner chromosomes (Hawley *et al*., 1994; Hassold and Hunt, 2001); and 3) it is more frequent with age in human oocytes, correlating with longer periods of meiotic arrest that have been suggested to lead to defects in some unknown aspect of a spindle-related mechanism (Hawley *et al*., 1994; Koehler *et al*., 1996; Lamb *et al*., 1996; Orr-Weaver, 1996; Hassold and Hunt, 2001). The reason so little is known about mechanisms of nondisjunction is that in many cell types, the process leading to it is difficult to study cytologically. The goal of the present study was to investigate the basis of nondisjunction during experimental arrest recovery in meiosis II crane fly spermatocytes, a cell type well suited for cytological analy-

This article was published online ahead of print in *MBC in Press* (http://www.molbiolcell.org/cgi/doi/10.1091/mbc.E06–10–0963) on February 21, 2007.

[V] The online version of this article contains supplemental material at *MBC Online* (http://www.molbiolcell.org).

Address correspondence to: Marie A. Janicke (mjanicke@buffalo.edu).

Abbreviations used: LC-PolScope, liquid crystal polarized light microscope.

Table 1. Comparison of incidence of anaphase lag at anaphase II 60 min into recovery with the incidence of nondisjunction at telophase II/cytokinesis 90 min into recovery

Duration of arrest	Incidence of anaphase lag (%)[a]	Incidence of nondisjunction (%)[b]
23–24 h	43 (of 475 anaphase II cells from 4 testes)	1 (of 595 telophase II/cytokinesis cells from 6 testes)
47–48 h	64 (of 2134 anaphase II cells from 8 testes)	3 (of 999 telophase II/cytokinesis cells from 13 testes)
72 h	72 (of 1692 anaphase II cells from 8 testes)	8 (of 485 telophase II/cytokinesis cells from 6 testes)

Data are based on analysis of fixed cell smears after cold arrests at 2°C for the indicated durations.

[a] Anaphase laggards defined in *Materials and Methods*.

[b] Data on cells that conform in all respects to that presented in Figure 1, G and I.

sis. Live-cell imaging with an LC-PolScope (Cambridge Research and Instrumentation, Woburn, MA) made it possible to directly observe kinetochore fibers of chromosomes whose subsequent behavior could then be followed.

We present in this report a newly observed mechanism for nondisjunction that involves neither failure of partners to lose cohesion nor premature loss of cohesion, but, rather, a spindle-related defect. The defects that we have discovered are monopolar and nearly monopolar malorientations of cohered sister chromosomes that are located near the equator at metaphase, disconnect at anaphase onset, and then are included during anaphase in the same nucleus as a result of malorientation, producing (n + 1) and (n − 1) daughter cells.

MATERIALS AND METHODS

Crane Fly Spermatocytes

A colony of crane flies (*Nephrotoma suturalis*) that is maintained in the laboratory year-round was the source of spermatocytes for this study. Secondary (meiosis II) spermatocytes were obtained from selected fourth instars and prepared for microscopy.

For live-cell specimens, testes were isolated from larvae in tricine insect buffer (Begg and Ellis, 1979), and they were ruptured under oil to make a spermatocyte culture that was viable for several hours. Two types of live-cell specimens were made. 1) Well preparations, typically used on inverted microscopes, were made by rupturing testes at the oil–glass interface of a well slide that was constructed as described by Janicke and LaFountain (1986). 2) "Sandwich" preparations, used with the high numerical aperture oil immersion lenses on the LC-PolScope (LaFountain and Oldenbourg, 2004), were made by rupturing testes under oil on a coverglass, which was subsequently mounted onto a glass microscope slide for observation.

For fixed cell specimens, testes were isolated as described above, but then their entire contents were smeared over the dry surface of a cover glass and fixed by air drying. Fixed cells were stained with 0.1 μg/ml Hoechst 33528 in 4% formaldehyde and then mounted on a microscope slide. Excess stain was blotted away, and the coverglass was sealed to the slide with nail polish.

Cold treatments for the induction of chromosome malorientation were performed as in previous studies (Janicke and LaFountain, 1982; LaFountain and Oldenbourg, 2004). For 2°C treatments, larvae were placed on refrigerated moist tissue paper in a Petri dish in the meat keeper of a refrigerator. For 0.2°C treatments, the Petri dish was put on an ice bath in the refrigerator. Recovery was in moist tissue paper at ~22°C.

Analysis of Anaphase Lag and Nondisjunction in Fixed Spermatocytes

Fixed cell specimens were used for assessing both the incidence of anaphase lagging and the incidence of nondisjunction in all of the spermatocytes contained within the population released from each of the testes studied. A systematic screening regimen was used by which the smeared contents of a testis were scanned manually back and forth from top to bottom while observing the contents in a phase-contrast microscope.

When the screen was for incidence of anaphase lagging, each late anaphase cell (in which the segregating chromosomes had not yet fused together upon reaching the poles) was scored according to whether any of the chromosomes were laggards. A laggard was defined as a chromosome that did not overlap along the long axis of the spindle with any of the properly segregating chromosomes. The results of such a screen are presented in Table 1 as percentage of all late anaphase II cells that contain laggards.

When the screen was for incidence of nondisjunction, the contents of a testis were scanned in a similar manner, but cells in which cytokinesis II was virtually complete were scored according to whether, based on the size difference of the two nuclei, the two daughter nuclei resulting from meiosis II seemed to have unequal numbers of chromosomes. Cells were not scored if cytokinesis was abortive or if they had chromatin either separate from the two daughter nuclei or extending equatorially from a daughter nucleus. Cells in which the two daughter nuclei seemed "balanced" were scored as normal (Figure 1F), and those in which the two nuclei seemed significantly different were scored as nondisjunction (Figure 1G). Results of this screen for nondisjunction are presented in Table 1 as percentage of otherwise normal cytokinesis II cells that show evidence for nondisjunction. To check the accuracy of this methodology, the locations of nondisjunction pairs were noted using the x-y coordinates of the stage vernier, so that they could be relocated for segmentation analysis. Nondisjunction was confirmed by quantitative fluorescence as described below.

Cytokinesis in fixed cells was scored as being successful if the cleavage furrow had constricted the cell in that area to <75% of the width of the cell at its widest point.

Microscopy

Fixed cells were analyzed using a Zeiss Photomicroscope II with transmitted phase contrast and epifluorescence optics. With both, a 40×/0.75 numerical aperture (NA) Neofluar objective was used to locate cells for screening and for segmentation analysis of selected cells undergoing cytokinesis to confirm nondisjunction that was detected by eye during the initial screening regimen. When screening necessitated just phase contrast optics, a Wild research stand with a 40×/0.75 NA Fluotar objective was used.

Data on chromosome malorientations and kinetochore fiber birefringence were obtained with the LC-PolScope, equipped with polarized light and DIC optics (60×/1.4 NA plan apochromat objective) used previously (LaFountain and Oldenbourg, 2004). A kinetochore fiber (Scarcello *et al*., 1986) is the bundle of microtubules that extends from the kinetochore to the pole; it contains kinetochore microtubules, which end at the kinetochore, and may contain a few nonkinetochore microtubules interspersed among the kinetochore microtubules. With the LC-PolScope, birefringence is revealed regardless of specimen orientation. *Z*-focus series were made at steps of 0.3 μm to maintain high spatial resolution.

Other live-cell observations were made with a Leica DMIRE2 with differential interference optics (60×/1.4 NA planachromatic objective). For these observations, anaphase II cells were imaged in time-lapse using a script that made a *Z*-focus series (0.5 μm steps) at each time point.

Image Acquisition and Analysis

Images of fixed cells were acquired in both phase contrast and fluorescence modes with a Princeton Instruments Micromax CCD camera and stored as TIFF files for subsequent analysis. In fluorescence mode, images of Hoechst-stained cells were used to determine differences in the DNA content of daughter nuclei. With both daughter nuclei in the same field of view, the exposure time was kept constant for the two daughter nuclei being compared by maximizing the 12-bit dynamic range for the brightest nucleus in the sample. Using IP lab software (Scanalytics, Fairfax, VA), the analysis of DNA content (based on Hoechst binding) of daughter nuclei was performed as follows. Boundaries of in-focus daughter nuclei were established by interactively segmenting the image until the segment precisely matched the area of the Hoechst-labeling. Densitometry was performed on the segmented images. Pixel values within each nucleus were summed and total pixel value was calculated for the Hoechst-labeled DNA within each nucleus.

For live-cell imaging, Z-series of well specimens were made with a Q-imaging RETIGA EXi camera on the Leica DMIRE2; the LC-PolScope was equipped with the same type of camera. All images were stored as TIFF files that were imported into either IP Lab or ImageJ (public domain software available from NIH: http://rsb.info.nih.gov/ij/index.html) for analysis.

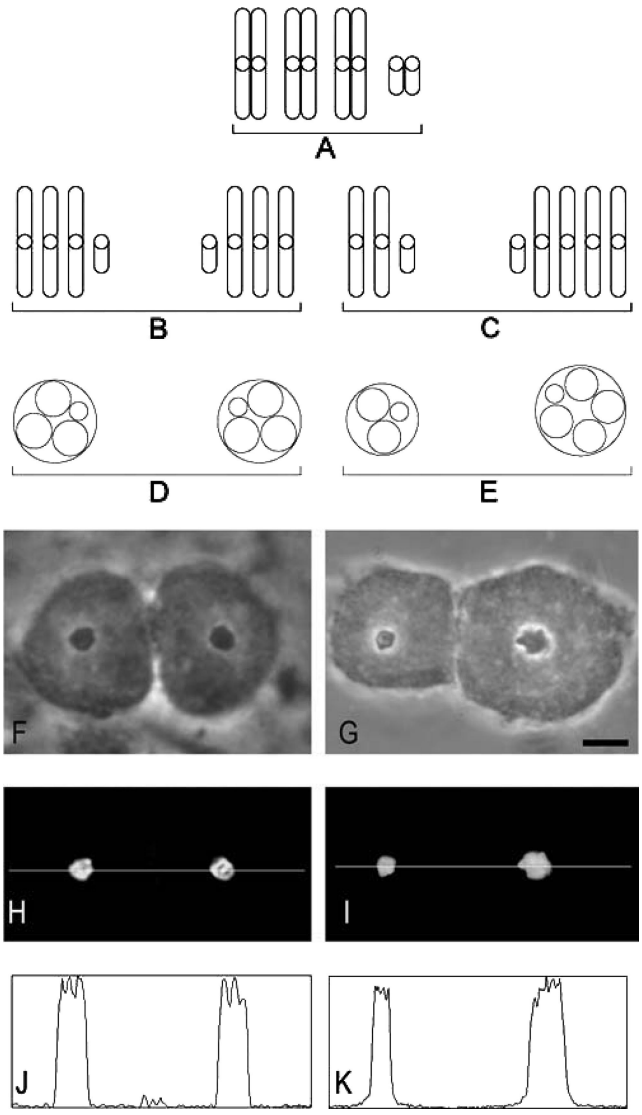

Figure 1. (A) Diagram of the karyotype of *N. suturalis*. Spermatocytes entering meiosis II have three metacentric autosomes and a small X or Y chromosome. (B and D) Normally, chromosome segregation during meiosis II produces two haploid daughter nuclei, each containing 50% of the chromatin. (C and E) One nondisjunction event produces one nucleus with just 35% and one nucleus with 65% of the chromatin. (F and H) Phase and Hoechst 33528 fluorescence images of an untreated control spermatocyte that has essentially completed cytokinesis after meiosis II. Daughter nuclei have similar sizes. (G and I) Images of a cold-recovering spermatocyte that has essentially completely cytokinesis after meiosis II. Its daughter nuclei display nondisjunction. The nucleus on the left seems smaller than the one nucleus on the right. The cell containing the small nucleus also is smaller. Bar, 5 μm. (J and K) Plots of fluorescence emitted along the lines drawn across the nuclei in H and I demonstrate similarities in size and fluorescence emitted from control nuclei and differences between the two cold-recovering daughters and between both cold-recovering daughters and control nuclei. Segmentation analysis (see *Materials and Methods* for details) of each of those nuclei demonstrated that the total pixel brightness of the two control nuclei differed by only 1%, whereas the difference between the two nuclei in Figure 3I differed by ~40%.

Time-lapse differential interference contrast (DIC) movies made with the Leica DMIRE2 (Leica Microsystems, Deerfield, IL) provided data on chromosome velocities, K-fiber lengths, and spindle lengths, all of which were obtained with the linear measurement tool included in IPLab software (Scanalytics, Fairfax, VA) and then imported into Microsoft Excel (Microsoft, Redmond, WA). With the LC-PolScope, the duration of intervals between Z-slices was irregular, due to the variation in the time spent calibrating the system between scans.

Birefringence retardation, also called retardance, in images made with the LC-PolScope was quantified by using a computer algorithm that computed retardance area within a domain of a selected kinetochore fiber as described previously (LaFountain and Oldenbourg, 2004). The program is built on the direct proportionality between the gray scale level (brightness) of a kinetochore fiber image in polarized light and the measured retardance within the fiber image. The retardance area is the integrated retardance across the fiber width and is directly proportional to the number of microtubules, with each microtubule contributing ~7.5 nm^2 to the retardance area of the fiber (Oldenbourg *et al*., 1998). Corrections are made for the angle of inclination of the kinetochore fiber with respect to the pole-to-pole axis of the spindle.

We estimate that the minimum number of bundled microtubules that is still detectable with the LC-PolScope in this study is three. This estimate is based on 1) the average fluctuations or noise of background retardance in LC-PolScope images of spermatocyte spindles and 2) the uniform fiber retardance that extends for at least several microns in the image. The morphologically distinct feature of an elevated retardance in an in-focus fiber section improves the detectability of the fiber above the noise background.

To depict the positions of different chromosomes that were imaged in different planes of a Z-focus series, an outline of the best in-focus image of each chromosome was traced using the pencil tool in Image J. The positions of the basal bodies were also marked. Tracings were stored as a separate image stack, which was then projected into a single plane. Afterward, the outlines of the maloriented chromosomes of interest in each two-dimensional (2-D) projection were highlighted by painting within the boundary of its tracing.

RESULTS

Crane fly spermatocytes entering meiosis II contain three morphologically indistinguishable metacentric autosomes and a small telocentric X or Y (Figure 1A). Each of the three autosomal dyads contains ~30% of the total chromatin, and the sex dyad contains ~10%. Thus, nondisjunction of just one pair of autosomal sisters increases the chromatin content of one daughter nucleus by 15% and decreases that of the other by 15% (Figure 1, B and C). That means an (n + 1) daughter would contain roughly twice the amount of chromatin (65% of the total) of that in an (n − 1) daughter (35% of the total) (Figure 1, D and E). Corresponding disparities in DNA content after staining with the DNA-specific fluorophore Hoechst 33528 (Figure 1, H–K) were readily detected by eye and quantified by fluorescence emission. Based on measurements made from 48 such pairs fixed during cold recovery (discussed below), the average nuclear diameter was 1.9 μm for the smaller nucleus of a pair and 2.6 μm for the larger (Figure 1, F and G). Screening for nondisjunction in fixed smears of control spermatocytes revealed no evidence for disparate daughter nuclei among 1470 cytokinesis II cells analyzed, indicating that baseline levels of nondisjunction are very low in this system, as they are in many other cells, including human fibroblasts (Cimini *et al*., 1999).

At metaphase II, each dyad is bioriented, having a birefringent bundle of ~30–40 microtubules—a kinetochore fiber—extending from the kinetochores of sisters to opposite poles (Figure 2A). This arrangement is called amphitelic orientation (Figure 3A). Dyads are stably positioned on the spindle equator and do not exhibit the oscillatory movements (directional instability) that are characteristic of chromosomes in mitotic cells (Skibbens *et al*., 1993). At anaphase onset, sister chromatids disconnect and kinetochore fibers shorten (anaphase A) over the course of ~10–15 min until sisters reach the edge of the polar centrosomes and poleward movement stops. Usually, all kinetochore fibers shorten at roughly the same rate (~0.5 μm/min), so segregating chromosomes reach the edge of the centrosomes at about the same time (Figure 2, B and C). As the chromosomes move poleward, the spindle elongates by 20–25% (Figures 2C and 3C and Supplemental Video 1). Spindle

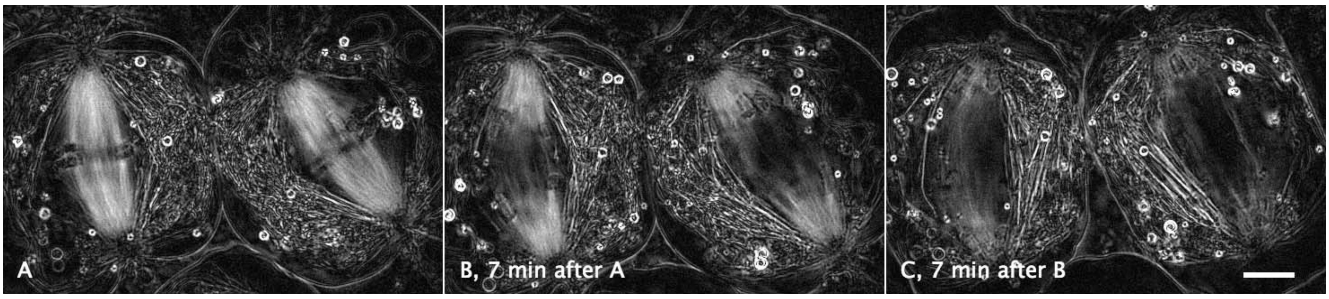

Figure 2. LC-PolScope images of anaphase of meiosis II in two crane fly secondary spermatocytes that originated from the same primary spermatocyte. Taken from the time-lapse movie in Supplemental Video 1. In LC-PolScope images and movies, image brightness expresses measured retardance independent of the orientation of the birefringence axis. White corresponds to 2.5 nm or larger retardance (retardance ceiling 2.5 nm). (A) Metaphase: dyad chromosomes are bioriented, exhibiting amphitelic orientation (Figure 3A) with birefringent kinetochore fibers extending from sisters to opposite poles (frame 2/60 of movie). (B) Midanaphase A: kinetochore fibers shorten and disjoined sisters move to opposite poles (frame 16/60 of movie). (C) Completion of anaphase A: poleward movement of sisters ceases upon their making contact with the polar centrosomes (frame 30/60 of movie). The spindle elongates during the course of anaphase A (concurrent anaphase B) as well as somewhat further subsequent to the completion of anaphase A. Bar, 5 μm. Time interval between frames of the movie is 30 s.

elongation (anaphase B) may continue somewhat even after anaphase A has been completed.

Overview of Meiosis II in Cold-recovering Spermatocytes

Previous work on meiosis I spermatocytes (Janicke and LaFountain, 1982) showed that exposure of crane fly larvae to cold (0.2–2°C) has two effects: 1) it causes existing spindles to depolymerize rapidly, and 2) it prevents assembly of spindles in spermatocytes entering meiosis after having undergone nuclear envelope breakdown in the cold. Both outcomes generate a condition we call cold-prometaphase, defined by absence of spindle microtubules and of random positioning of chromosomes in the cytoplasm. When cold-prometaphase I spermatocytes are returned to room temperature, they assemble prometaphase I spindles rapidly, and bivalents become oriented and congress to a metaphase I plate; anaphase I begins at ~60 min of recovery, and at mid-to-late anaphase (90 min of recovery), there is a high incidence of anaphase lag. With longer cold arrests, more cells accumulated in cold-prometaphase I due to nuclear membrane breakdown in the cold, and frequencies of anaphase lag were high in those cells when they reached anaphase (Janicke and LaFountain, 1982, 1984).

Here, we found the same is true for meiosis II. When cells arrested in cold-prometaphase II were returned to room temperature, they assembled spindles rapidly, allowing dyads to become attached to microtubules rapidly, they began anaphase II at ~35 min of recovery, and, when they reached late anaphase II at 60 min of recovery, they had a high incidence of anaphase lag. With longer cold arrests, larger numbers of cold-prometaphase cells accumulated. These were likely made up of a small fraction of cells that had regressed from prometaphase II (with a spindle) to cold-prometaphase II upon exposure to cold as well as a larger fraction of cold-prometaphase cells that had been in interkinesis in the cold and had undergone nuclear envelope breakdown in the absence of spindle formation. Anaphase II was completed by ~60 min of recovery and cytokinesis at ~90 min of recovery. The time course of meiosis II during cold recovery closely paralleled that in untreated control cells, except that a slightly longer period (45 min compared with 35 min for cold recovery) elapses in untreated cells between the onset of prometaphase II (at nuclear membrane breakdown) and the beginning of anaphase II.

Chromosome Segregation during Meiosis II in Cold-recovering Spermatocytes

A chromosome was scored as a laggard if it was located at late anaphase far enough behind the properly segregating chromosomes that it did not overlap with them. It is important to note that there is no one standardized definition of anaphase lag. Some consider a chromosome to be a laggard only if it remains immobilized in the interzone, not included in either daughter nucleus, becoming a micronucleus. Others, including us, define a laggard by its anaphase position relative to nonlaggard chromosomes, irrespective of its ultimate fate. In our material, many anaphase laggards shifted poleward to become included within daughter nuclei (also see Falck *et al*., 2002). For example, after 72 h at 2°C, 72% of anaphase II cells had laggards (Table 1). At 90 min of recovery after the same cold treatment, only 24% had distinct laggards in the interzone (i.e., micronuclei), whereas 38% had chromatin that trailed from a daughter nucleus equatorially, deriving from former laggards that had fused with a daughter nucleus but had not been compactly included. Hence, the frequency of micronuclei was substantially lower than the frequency of lagging using our scoring criteria.

Any chromosome and any number of chromosomes could lag in cold-recovering meiosis II. The incidence of laggard induction correlated with the duration of cold arrest, data for 2°C exposures being given in Table 1. Data for 0.2°C were similar. At 60 min of recovery after 1-d exposures to 2°C, 43% of anaphase cells had one or more laggards, but at 60 min of recovery after 2–3 d at 2°C, the majority of anaphase II cells (64–72%) had laggards. In untreated cells, laggards are found in only 5% of anaphase cells.

We applied the term "nondisjunction" only to examples that conformed in all respects to Figure 1, F–I: daughter nuclei were compact and disparately sized, there was no evidence of a micronucleus, and the cell had essentially completed cytokinesis to form two daughter cells that were still contiguous. Of such cells fixed at 90 min of recovery, the percentage that had daughter cells with at least a 2:1 disparity in nuclear size was 1% after 1-d exposures to 2°C, 3% after 2 d, and 8% after 3 d (Table 1). Thus, the incidence of nondisjunction was low in comparison with that of anaphase lagging, but it increased with increased duration of cold treatment.

To assess the impact of the induced anomalies on cytokinesis, we analyzed fixed cells, because in live-cell oil prep-

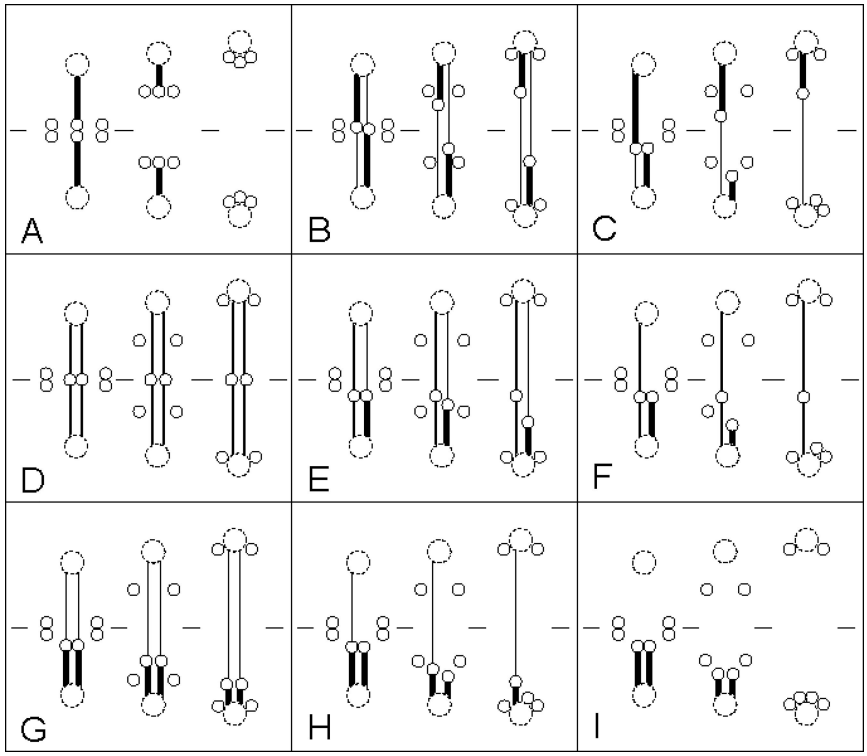

Figure 3. Diagrams of various types of meiosis II dyad orientations observed in untreated (A) and in cold-recovering (A–I) spermatocytes and fates of chromosomes derived from them. Normal chromosome distribution results from the orientations in (A–C), whereas in (D–F) anaphase laggards remain near the plane of the cleavage furrow, and in G–I the outcome is nondisjunction. Horizontal lines indicate the plane of the spindle equator. Dashed circles represent polar centrosomes, open circles represent kinetochores (chromosomes arms are not shown), and vertical lines are kinetochore fibers. Thickness of the fiber signifies its level of brirefringence in comparison with the other fibers. Kinetochore fibers are drawn only for the central dyad; the other kinetochores are shown as they would behave if they exhibited normal amphitelic orientation (A). Depictions of kinetochore fiber shortening, lengthening, and spindle elongation do not attempt to quantify exactly how these parameters changed but only give qualitative general illustrations of how positions of kinetochores and spindle poles changed relative to one another. The number of cells recorded in each category is indicated, but it does not reflect the actual frequency of different orientations in the population, because cells were not recorded at random, but rather they were selected because of our interest in the particular behavior their chromosomes were displaying. (A) Amphitely: the normal orientation for meiosis II found in all untreated spermatocytes that were studied (an example being illustrated in Figure 2) and in normally segregating chromosomes of all cold-recovering spermatocytes studied. (B) Meroamphitely with merotely in both kinetochores: (recorded in 3 cells; 1 cell first observed at early anaphase, and 2 cells first observed at midanaphase). The less birefringent fiber of each laggard elongated via anaphase B. As the initial positions of both laggards was at the equator, both shifted away from the equator into opposite half-spindles (with limited kinetochore fiber shortening), so that laggards were included within opposite daughter nuclei. (C) Meroamphitely with merotely in one kinetochore: (recorded in 5 cells; 1 cell first observed at anaphase onset [cell 99; Figure 6], 1 cell first observed at early anaphase, and 3 cells first observed at midanaphase). (D) Balanced merotely in both kinetochores: (recorded in 1 cell first observed at midanaphase). Both kinetochore fibers of each sister elongated, and the laggards remained at the equator. (E) Balanced merotely in one kinetochore and unbalanced merotely in the other: (recorded in 5 cells; 1 cell first observed at metaphase, 3 cells first observed at anaphase onset, and 1 cell first observed at midanaphase). The unbalanced merotelic moved away from its less birefringent fiber and hence away from the equator, whereas the balanced merotelic made no progress from its starting position. (F) Balanced merotely in one kinetochore and nonmerotely in the other: (5 examples recorded in 4 cells; 1 cell first observed at anaphase onset and 4 cells first observed at midanaphase). Both fibers of the merotelic elongated as it remained near its starting point, slightly closer to the pole to which its nonmerotelic sister moved. (G) Syntely with merotely in both kinetochores: (3 examples recorded in 2 cells; all 3 cells first observed at metaphase). The dyad began anaphase nearer to one pole. Neither chromatid moved all the way to the pole during anaphase. (H) Merosyntely with merotely in one kinetochore: (recorded in 2 cells, both cells first observed at metaphase, including cell 125 [Figure 5]). (I) Syntely without merotely: (recorded in 6 cells, all cells first observed at metaphase, including cell 132 [Figure 4]).

arations, cytokinesis commonly fails even without treatment. Cytokinesis was scored as successful in fixed cells if the cleavage furrow had constricted the equator at least 75% (as in Figure 1F). We found success rates of 90% in cytokinesis II cells from untreated larvae and 86% in normal cold-recovering telophase II cells (with balanced, compact daughter nuclei and no micronuclei) fixed at 90 min of recovery after 72 h at 2°C. At the same recovery time from the same cold exposure, cytokinesis was scored as successful in only 3% of the cells that had micronuclei and no other anomalies. These results show that, of the laggards that became micronuclei, the majority inhibited cytokinesis and hence likely led to production of cells with diploid chromosome complements rather than aneuploid cells. Of 72-h–arrested 90-min–recovered telophase II displaying only nondisjunction, 80% were scored as successfully cleaving (Figure 1G) (contrast Shi and King, 2005). Thus, the successful completion of cytokinesis seems to be more affected by the presence of chromatin at the equator than by imbalance in chromosome numbers at the two poles (also see Weaver *et al*., 2006). About half the cells with chromatin trailing equatorially from a daughter nucleus were scored as aborting cytokinesis.

To compare the contribution of lagging versus nondisjunction to aneuploidy, we considered only cells that were cleaving successfully. After 90 min of recovery from 72 h of cold, only 1% of cleaving otherwise normal telophase cells had micronuclei (still discrete laggards), compared with the 8% that exhibited nondisjunction. We have no evidence that those micronuclei either disintegrated or were lost, but it is possible that they resulted in some (n + 1) spermatids. Thus, nondisjunction seems to have contributed more to aneuploidy than did chromosome loss (also see Cimini *et al*., 1999).

Chromosome Malorientation as a Cause of Lagging and Nondisjunction

All anomalous segregation observed by live-cell imaging with the LC-PolScope was attributable to chromosome malorientation. That is, recovering dyads had a high probability for making improper connections with the two spindle poles, and those malorientations resulted in anaphase lag

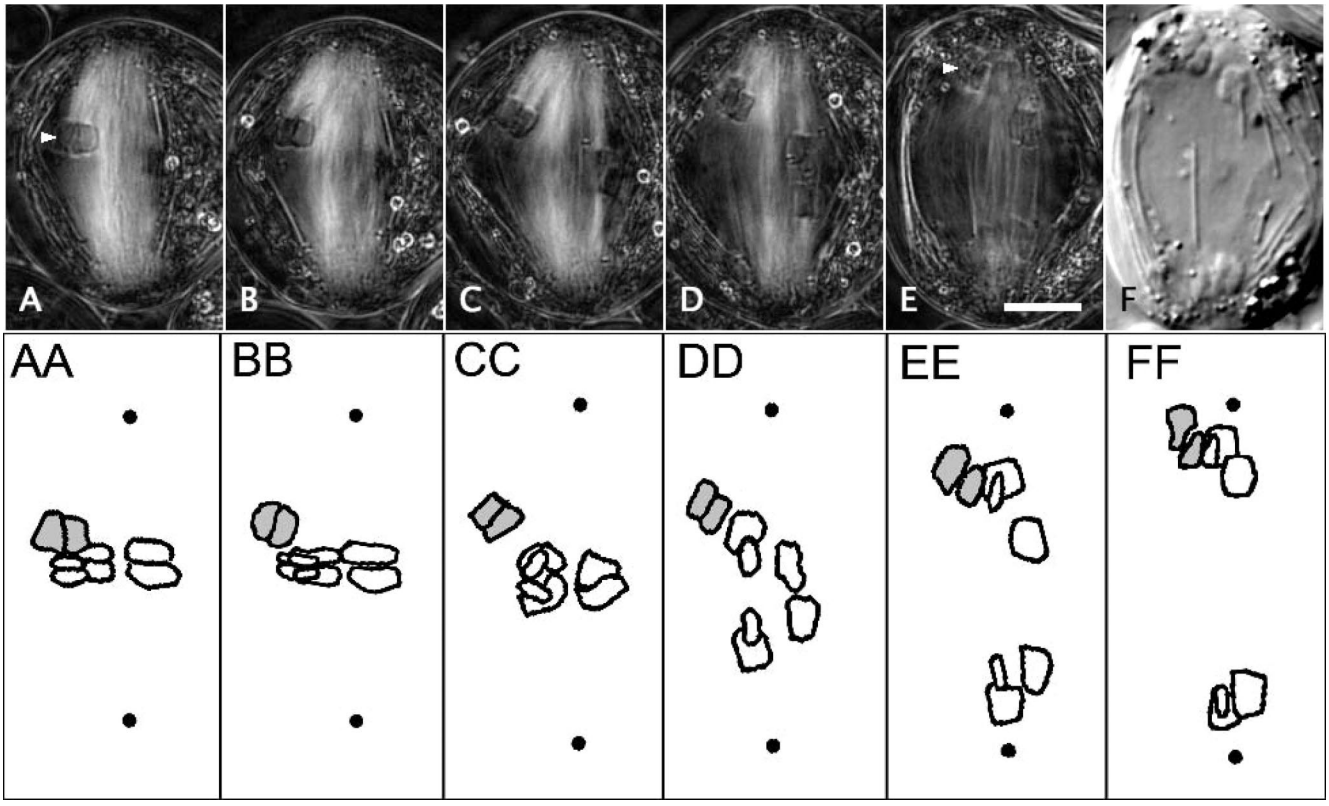

Figure 4. Syntelic orientation of sisters that cosegregate to the same pole during anaphase A (cell 132). Cold treatment: 72 h at 2°C (retardance ceiling 2.5 nm). (A) Twenty-one minutes into recovery: at metaphase, the syntelic dyad (arrowhead) is at the left periphery of the spindle. Both kinetochores have robust kinetochore fibers (97 kinetochore microtubules for the pair; see Figure 7A, compare with Table 2) oriented to the upper pole. The kinetochore fibers of this dyad are tilted away from the spindle axis more than the fibers of the bioriented chromosomes. This is best visualized by viewing the Z-focus series made with this cell, provided in Supplemental Video 2. Also note in the video the absence of birefringence on the equatorial side of the syntelic dyad, offering no evidence for merotely. (B) Twenty-eight minutes into recovery: anaphase begins. The separation of the two chromatids of the syntelic dyad is resolved as they move poleward, and the left-most kinetochore of the syntelic dyad advances poleward slightly ahead of the other kinetochore. (C and D) Thirty-four minutes and 41 min into recovery: continuation of anaphase A and the shortening of syntelic kinetochore fibers. (E) Forty-nine minutes into recovery: cosegregating sisters (arrowhead) reach the spindle pole. (F) Sixty-one minutes into recovery: DIC image of four autosomes that segregated to the upper pole and just two autosomes segregated to the lower pole. Bar, 5 μm. (AA–FF) 2-D projections (see *Materials and Methods*) of the Z-focus series containing the images presented in A–F show metaphase and anaphase positions of all of the chromosomes in cell 132. Dots locate basal bodies within the polar centrosomes. (AA) Twenty-one minutes into recovery: at metaphase, the syntelic dyad (painted gray) is positioned slightly off the equator. (BB) Twenty-eight minutes into recovery, anaphase begins. (CC and DD) Thirty-four and 41 min into recovery: cosegregation of syntelic sisters to the same pole. (EE as in E and FF as in F) The outcome is nondisjunction.

and nondisjunction. All laggards that were studied exhibited merotelic orientation, i.e., the single kinetochore of the laggard had kinetochore fibers connecting it to both spindle poles (Figure 3, B–H), a malorientation first documented at anaphase in crane fly meiosis I spermatocytes recovering from cold (Janicke and LaFountain, 1984) or from microtubule inhibitors (Ladrach and LaFountain, 1986). Thus, a laggard's failure to move properly to one of the poles was caused by its having another kinetochore fiber to the opposite pole (see also Cimini *et al*., 2001).

The only chromosomes observed to undergo nondisjunction were those that were oriented either syntelically, meaning sisters had their kinetochore fibers directed toward the same pole (Figures 3I and 4), or merosyntelically, meaning near-syntelic orientation but with one or both kinetochores having a second, less robust fiber directed toward the opposite pole (Figures 3, G and H, and 5). Direct observation of these malorientations causing nondisjunction (Figures 4, AA–FF, and 5, AA–EE) is a new finding with several remarkable features.

Quite significant is that we observed syntelic dyads that were positioned near the spindle equator at metaphase (Figure 4, A and B) and that did not exhibit either oscillatory behavior (Skibbens *et al*., 1993) or orientation instability (Henderson *et al*., 1970). Although shorter at metaphase than those of amphitelic dyads in the same cells, syntelic kinetochore fibers were robust (Figure 7A and Table 2), containing similar numbers of microtubules as amphitelic fibers in the same cell, and upon disjunction of sisters at anaphase onset, they exhibited anaphase A shortening (Figure 4, C–F, and AA–FF) just like that of amphitelic fibers. Because syntelic dyads were somewhat closer at metaphase to the pole to which they were oriented, their chromatids in many cases preceded the other chromosomes in making contact with the centrosomes.

The pathway to nondisjunction by sisters from merosyntelic dyads (Figures 3, G and H, and 5, A–E and AA–EE) was different from that of sisters from syntelic dyads. In merosyntely, shortening of the leading kinetochore fiber of the merotelic kinetochore(s), and hence, poleward movement of

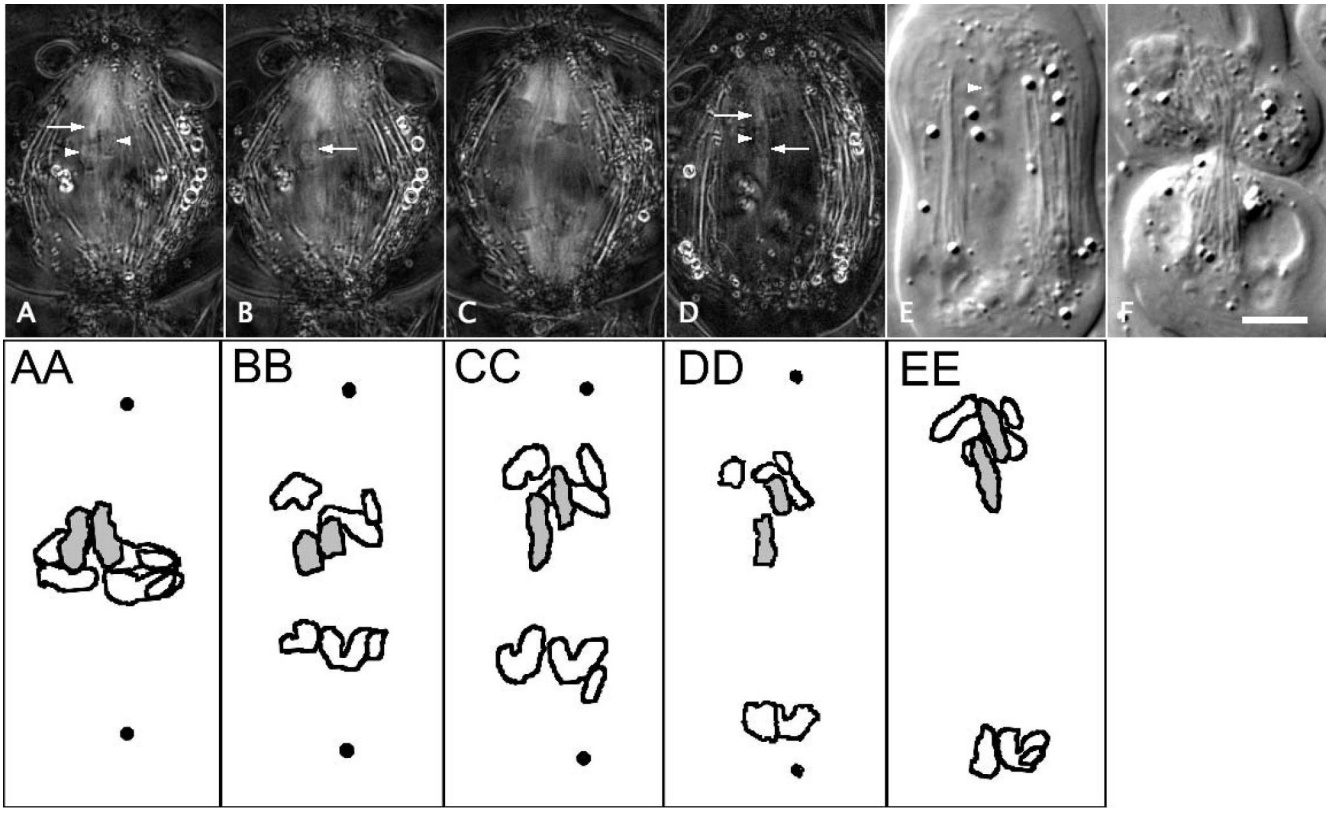

Figure 5. Merosyntely in cell 125 causes nondisjunction. Cold treatment: 72 h at 2°C (retardance ceiling 2.5 nm). (A–C) Thirty-two minutes into recovery: anaphase onset in three slices taken from the Z-focus series that is supplied as Supplemental Video 3 to illustrate the behavior of chromosomes from a merosyntelic dyad (in A and B) and two other chromosomes that come from properly bioriented dyads and are segregating normally (in C). (A) Slice 7/27. (B) Slice 8/27. (C) Slice 15/27. (A and B) The right-side daughter (left-pointing arrowhead) is not merotelic and is closer (~7.2 μm) to the upper pole than the merotelic kinetochore of the left-side sister (right-pointing arrowhead), which is ~7.8 μm from that pole. The merotelic kinetochore has 33 microtubules (right-pointing arrow) extending to the upper pole (Figure 7B) and 15 microtubules (left-pointing arrow) extending to the lower pole (Figure 7C). (D) Forty-four minutes into recovery: anaphase progresses with nonmerotelic chromosomes approaching the pole. In the merotelic chromosome (right-pointing arrowhead), both its more birefringent fiber (right-pointing arrow), to the closer pole, and the long less birefringent fiber (left-pointing arrow), to the distal pole, have elongated in the time interval after A and B above, the former by less than a micrometer (~0.8 μm), whereas the less birefringent fiber elongated 4–5 times that (~3.8 μm). Importantly, the merotelic sister is still located in the same half-spindle as its properly segregating sister. (E) Fifty-four minutes into recovery: DIC image upon the initiation of cytokinesis. The merotelic sister (arrowhead) is near the group of chromosomes that reached the spindle pole, but the merotelic sister does not make contact with the polar centrosome as normally segregating chromosomes do. (F) Ninety-six minutes into recovery: cytokinesis is well underway. The merotelic sister is included in the same (n + 1) nucleus as its sister. Bar, 5 μm. (AA–EE) 2-D projections of Z-focus series of cell 125 illustrate merosyntely causing nondisjunction. (AA) From Z-focus series at anaphase onset at 27 min into recovery. Chromosomes derived from the merosyntelic dyad are painted gray. (BB) Thirty-two minutes into recovery as in A–C. (CC) Thirty-five minutes into recovery. (DD) Forty-four minutes into recovery as in D (sex chromosome at lower pole was not included in the Z-focus series.) (EE) (n + 1) chromosomes are at the upper pole, and (n − 1) chromosomes are at the lower pole as in E (polar centrosomes could not be located).

the kinetochore, was inhibited compared with that of nonmerotelic chromatids segregating to the same pole (Figure 5, A–C and AA–EE). During the late stages of anaphase, lengthening of the trailing fiber, always the less birefringent of the two fibers of the merotelic kinetochore (Figures 5, A and B, and 7, B and C), allowed the merotelic to move far enough away from the equator to fuse with the chromosomes of the nucleus that contained its sister (Figure 5, D–F). The merotelic initially extended from the nucleus in the direction of the equator before becoming more compactly included. Because a merosyntelic dyad was closer to its pole at metaphase than an amphitelic dyad (Figure 5AA), the nonmerotelic chromatids started out behind the merotelic chromatids but then passed them (Figure 5, CC–EE). Thus, a merotelic chromatid from a merosyntelic dyad never was far enough behind the nonmerotelics to be scored as a laggard by our criteria (see *Materials and Methods*), although it never fully reached the centrosome (Figure 5E and EE).

We reported previously that a bundle of <10 microtubules might not be detected with the LC-PolScope (LaFountain and Oldenbourg, 2004), but we have revised that lower limit to be less than three microtubules in images recorded for this study (see *Materials and Methods*). We therefore questioned whether the observed syntelic dyads, despite having only one birefringent fiber extending from each kinetochore, might have one or two undetected microtubules extending from them toward the opposite pole. The behavior of the chromosomes we are calling syntelics argues in three ways against their having undetected, oppositely directed microtubules. 1) Anaphase A movement is impaired in merotelic chromatids. We know from previous electron microscopy analysis of meiosis I laggards that just one merotelic kinet-

Table 2. Comparison of data regarding kinetochore fibers in control versus cold-recovering meiosis II spermatocytes

	Control spermatocytes Only amphitelic orientation	Cold-recovering spermatocytes		
		Cells having only amphitelic orientations	Amphitelic orientations in cells with a syntelic dyad	Syntelic dyads
Avg length (μm)[a] of metaphase kinetochore fibers	8.9 ± 0.9 (n = 86)	7.3 ± 0.7 (n = 13)	7.8 ± 0.6 (n = 34)	6.1 ± 0.8 (n = 12)
Tilt angle (degrees) of kinetochore fiber relative to pole-to-pole axis	8.6 ± 4.3 (n = 14)		7.0 ± 3.9 (n = 19)	26.8 ± 10.8 (n = 6)
Microtubules/kinetochore[b]	37.5 ± 8.1 (n = 17)		53.2 ± 13.1 (n = 9)	50.3 ± 10.0 (n = 3)

[a] Distance from kinetochore center to basal body at the core of the centrosome.

[b] From retardance area analysis (see Figure 7).

ochore microtubule can cause a chromosome to trail behind the others at anaphase (LaFountain, 1985). In contrast, chromatids from syntelic dyads moved poleward at the same time and same approximate velocity as properly oriented chromosomes, sometimes reaching the pole before properly oriented chromosomes. 2) Because their leading fibers do not shorten substantially during anaphase, merotelic chromosomes do not make actual contact with the centrosome even after anaphase spindle elongation. In contrast, the length of kinetochore fibers of syntelics shortened to zero as the chromatids of syntelics moved all the way to the centrosome. 3) At metaphase, we have observed only central locations and shallow tilt angles of 15° or less for bioriented dyads (Figure 3, A–H, and Table 2), including merosyntelics (Figure 3, G and H), the merosyntelic dyad in Figure 5 being tilted only 7° relative to the pole-to-pole axis. In contrast, syntelic dyads were positioned at the spindle periphery with kinetochore fiber tilt angles ranging between 18 and 47° (Figure 4A and Table 2), consistent with their not being subject to forces focused toward the opposite pole. Even a single kinetochore microtubule extending toward the opposite pole has been reported to be capable of exerting force toward that pole (McEwen *et al*., 1997). The difference between the tilt angle of syntelic kinetochore fibers and the fibers of other chromosomes in the cell also suggests that the kinetochores of syntelics were not interacting laterally with other kinetochore fibers to achieve congression (Kapoor *et al*., 2006).

The Full Spectrum of Malorientations and the Ultimate Fate of Laggards

Like merotelic chromatids from merosyntelic dyads (Figure 3, G and H), other merotelic chromatids (Figure 3, B–F) also failed to reach the polar centrosomes, and when they were included in a daughter nucleus, it was only because they were close enough to nonmerotelics to fuse with them at telophase. Unlike merotelic chromatids from merosyntelic dyads, the merotelic chromatids in Figure 3, B–F were, at some point in anaphase, far enough behind the nonmerotelics to be scored as laggards by our criteria.

If the two fibers of a merotelic had approximately equal birefringence (Figure 3, D–F), then both fibers elongated. This resulted in little or no net anaphase movement of the laggard away from the equator at anaphase, as also reported by Cimini *et al*. (2004).

Laggards that had one fiber that was more birefringent than the other (unbalanced merotely; Figure 3, B, C, and E) behaved as described for merotelics from merosyntelic dyads: shortening of the kinetochore fibers of merotelics was greatly impaired during anaphase, but the less birefringent kinetochore fiber elongated along with the separation of the two poles When both sisters were merotelic (Figure 3B) and the dyad was meroamphitelic (almost amphitelic but with some merotely), dyads were near the equator at metaphase. Their sister chromatids moved away from the equator toward opposite poles during anaphase spindle elongation, but they were far enough behind the nonmerotelics to be scored as laggards. One meroamphitelic dyad was observed that had merotely in just one kinetochore (Figure 3C). The dyad was located at metaphase in the half-spindle of the less birefringent fiber of the merotelic (Figure 6, A, B, and AA). Lengthening of the less birefringent fiber of the merotelic therefore caused the initial direction of the anaphase movement of the merotelic to be toward, rather than away from, the equator. The merotelic then moved slightly beyond the equator and into the opposite half-spindle (Figures 6, C and DD, and 7, D and E), where it was still lagging when cytokinesis began. Movement toward the equator at anaphase is an unusual finding that may relate to results reported by Pidoux *et al*. (2000) in yeast. It confirms that the direction of anaphase B shifting does indeed depend on relative robustness of kinetochore fibers (Cimini *et al*., 2004) and not on the half-spindle in which a merotelic begins anaphase. Importantly, whether the merotely was in one or both kinetochores, meroamphitely (Figure 3, B and C) always resulted in sisters moving away from one another.

Ruling Out Other Potential Causes of Nondisjunction

To evaluate whether factors other than malorientation may have contributed to the incidence of nondisjunction in fixed cell smears, we investigated four known alternative sources of aneuploidy, and all were ruled out, as follows. 1) Multipolar spindles. Had cold exposure of secondary spermatocytes caused them to form tripolar or tetrapolar spindles during recovery, (n + 1) and (n − 1) daughter nuclei may have resulted. To test this, meiosis II cells were analyzed from testicular contents fixed at recovery times (60 min) too short for them to have been in meiosis I during exposure. Frequencies of multipolar anaphase II spindles were similar to those in untreated smears. 2) Sticky sisters. We found no evidence for intact dyads at any postmetaphase II stage. 3) Precocious disjunction of sisters. Smears of cells were fixed when the "wave" of meiosis II cells peaked at metaphase II (45 min of recovery), and other smears were made of cells fixed in the cold without recovery. Of 1553 metaphase II cells, only three cells had what seemed to be a pair of disjoined sisters. None of the dyads in cold-prometaphase II seemed to have precociously disjoined. 4) Chromosomes

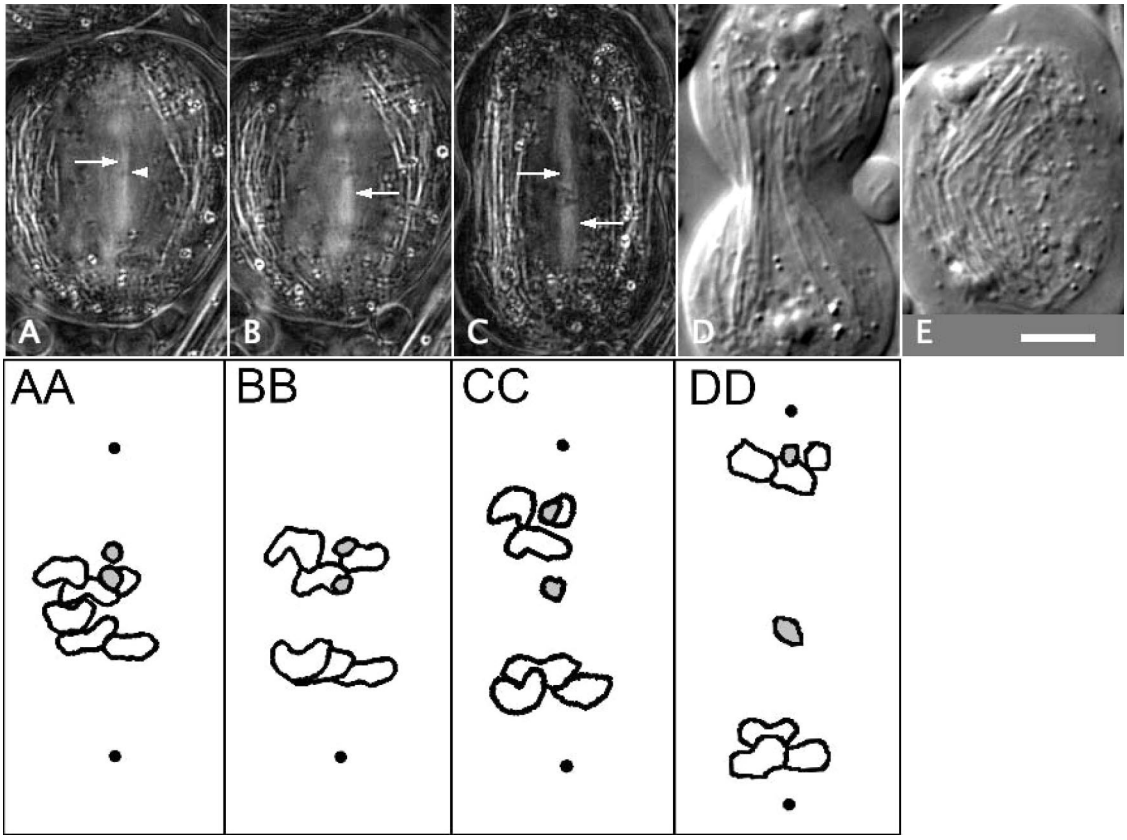

Figure 6. A meroamphitelic sex dyad that exhibited merotely in one of its two kinetochores in cell 99. The merotelic chromosome moves toward the equator as the spindle elongates and its less birefringent fiber lengthens. Neither of its kinetochore fibers shortens. Cold treatment: 75 h at 2°C. (retardance ceiling 2.0 nm). Anaphase begins 27 min into recovery, and first measurements of kinetochore fibers at 31 min into recovery (see AA) indicate the merotelic kinetochore is ~7.9 μm from the upper pole and ~9.4 μm from the lower pole. (A and B) Forty minutes into recovery: two slices from a Z-focus series of cell 99 illustrate kinetochore fibers of the merotelic sex chromosome (arrowhead). (A) Slice 20/38. (B) Slice 22/38. The fiber to the lower pole (left-pointing arrow) contains 37 microtubules (Figure 7D), whereas the fiber to the upper pole (right-pointing arrow) contains 24 microtubules (Figure 7C). With the progression of anaphase, the merotelic chromosome moved toward the equator as the less birefringent fiber elongated. (C) Forty-eight minutes into recovery: as anaphase progresses, the merotelic laggard shifts past the equator and into the lower half-spindle. The less birefringent fiber (right-pointing arrow) is now ~3.4 μm longer than at anaphase onset, whereas the length of the more birefringent fiber (left-pointing arrow) has increased only ~0.4 μm during the same interval. (D) Sixty-seven minutes into recovery: cytokinesis begins. (E) Ninety-four minutes into recovery: cytokinesis fails. Bar, 5 μm. (AA–DD) 2-D projections of chromosome positions in cell 99. (AA) Thirty-one minutes into recovery: at anaphase onset, sisters derived from the meroamphitelic sex dyad (painted gray) are positioned in the upper half-spindle. (BB) Thirty-four minutes into recovery: one of the sex sisters exhibits anaphase lag as its sister moves to the upper pole. (The upper centrosome was not included in the Z-focus series.) (CC) Thirty-nine minutes into recovery: the laggard is positioned near the equator. (DD) Forty-eight minutes into recovery: the laggard is positioned in the lower half-spindle.

"stuck" at the poles. Very few metaphase II cells (2/985) were found with an off-equator dyad after 44-h exposures, whereas more (64/565 cells) were found during recovery from 72 h. Off-equator dyads were not observed adjacent to the pole as would have been expected if forces that act away from the pole were inoperative (Weaver *et al*., 2006). Instead, they were in positions similar to those of maloriented dyads in our live-cell preparations.

DISCUSSION

Cold-recovering meiosis II spermatocytes displayed a spectrum of chromosome orientations, from fully monopolar to fully bipolar. Only syntelic (fully monopolar) and merosyntelic (nearly monopolar) orientation caused nondisjunction.

Monopolar orientations normally are detected and corrected by mechanisms (Shannon and Salmon, 2002; Biggins, 2004; Gassmann *et al*., 2004; Maiato *et al*., 2004) that cause anaphase to wait for achievement of bipolar orientations and that, if disrupted, cause monopolar chromosomes to be "stuck at the poles" (Kline-Smith *et al*., 2004). Tension, usually achieved through bipolar orientation, is thought to be necessary for chromosomes to maintain their orientation, achieve full microtubule complements, keep from moving to a pole before anaphase, and inactivate the anaphase checkpoint (Nicklas, 1997). Although cold-recovering syntelics are monopolar, they had metaphase positions away from the poles, had robust kinetochore fibers of sizable length, and did not delay anaphase. We suggest these syntelics did experience tension, not from oppositely directed kinetochore fibers but from polar ejection forces that counteracted the poleward forces of their kinetochore fibers. In crane fly spermatocytes, transverse equilibrium forces move acentric fragments to the spindle periphery, where they are driven equatorially by polar ejection forces hypothetically involving a yet-to-be-characterized kinesin-10 orthologue (i.e.,

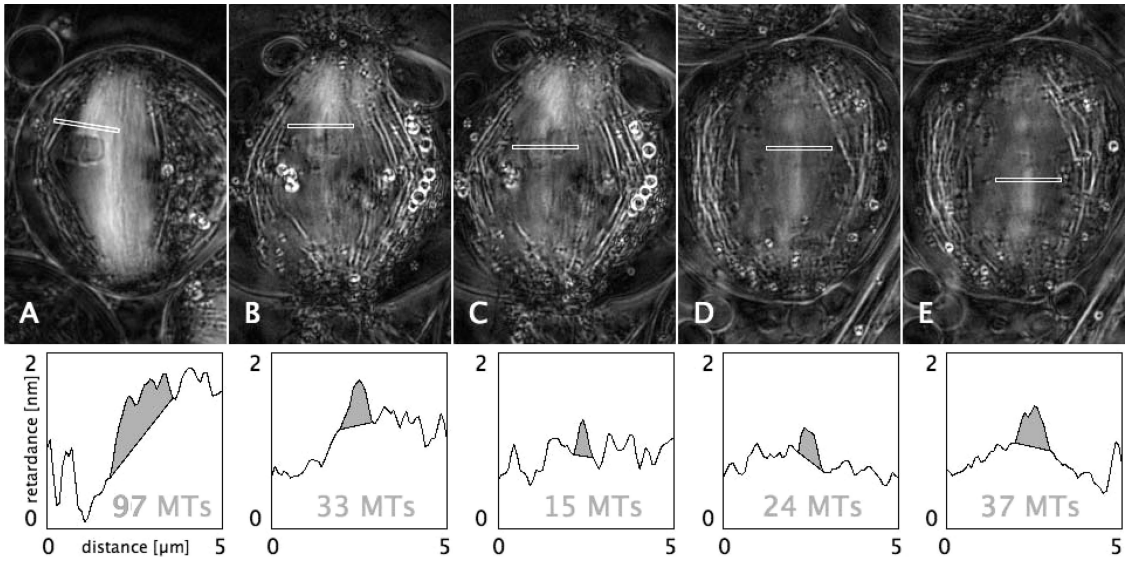

Figure 7. Duplicate images of maloriented chromosomes depicted in Figures 4–6 to illustrate how the retardance area data were obtained (retardance ceiling 2.5 nm) (A) The selected portion of slice 14/28 from cell 132 (presented as Figure 4A) was analyzed using an algorithm (described in detail by LaFountain and Oldenbourg, 2004) to generate a plot of retardance (in units of nanometers) as a function of distance (micrometers). A line scan having the shape of an elongated rectangle 5 μm long by 4 pixels wide was made perpendicular to the kinetochore fiber(s) of interest. The portion of the scan corresponding to the kinetochore fiber(s) was identified (the shaded area in the plot). The area under that portion of the plot is the retardance area (in units of square nanometers) of the selected kinetochore fiber(s). The conversion factor from retardance area to number of microtubules is 7.5 nm^2/microtubule (MT), yielding an apparent value of 96 microtubules for the two kinetochore fibers from this syntelic dyad. Because these fibers were inclined somewhat (by ~4°) in relation to the x-y plane of the image, computed retardance area was adjusted to take that into account (see LaFountain and Oldenbourg, 2004), yielding an actual value of 97 microtubules in these two fibers. (B and C) Likewise, retardance area analysis was performed on slice 7/27 (presented as Figure 5A) and on slice 8/27 (Figure 5B) of the merotelic sister that was derived from the merosyntelic dyad in cell 125, revealing 33 microtubules in the fiber extending from the merotelic to the upper pole and 15 microtubules in the fiber extending to the lower pole. (D and E) Slice 20/38 (presented as Figure 6A) and slice 22/38 (Figure 6B) from a Z-focus series of the merotelic sex chromosome in cell 99 were similarly analyzed, revealing a less birefringent fiber containing 24 microtubules to the upper pole and a more birefringent fiber containing 37 microtubules to the lower pole.

chromokinesin) on chromosome arms (LaFountain *et al*., 2002). Regardless of where cold-recovering dyads were at recovery onset (undetermined due to time lost in specimen preparation), failure to biorient should locate them at the spindle periphery and then ejection forces would drive them toward the equator at an angle parallel to peripheral microtubules lying at steep angles to the pole-to-pole axis. Accordingly, cold-recovering syntelics were at the periphery and had tilted kinetochore fibers.

Failure of syntely to elicit a wait-anaphase response may be a peculiarity of this cell type (LeMaire-Adkins *et al*., 1997; Forer and Pickett-Heaps, 1998) or of cold recovery (but see Cimini *et al*., 2002). Alternatively, the anaphase checkpoint may be satisfied by the full kinetochore microtubule occupancy of these syntelics and/or by the tension exerted by polar ejection forces on them (Cimini and Degrassi, 2005; Pinsky and Biggins, 2005). At anaphase, kinetochore fibers of syntelics shortened in concert with those of normally oriented chromosomes, presumably because proteolysis of chromokinesins (Antonio *et al*., 2000; Funabiki and Murray, 2000) allowed their chromatids to move poleward after loss of cohesion.

Meroamphitely (Figure 3, B and C) does not cause nondisjunction. This is despite the fact that, probably because it is bipolar, merotely does not trigger a wait-anaphase response (Cimini *et al*., 2002). If merotely escapes the preanaphase orientation correction mechanism, it then encounters a second mechanism (Cimini *et al*., 2003) to help prevent it from causing aneuploidy. That second mechanism is anaphase B. During anaphase B, merotelics follow "Cimini's rules" (Cimini *et al*., 2004; Salmon *et al*., 2005): 1) their kinetochore fibers shorten little, but 2) their less robust fiber lengthens with spindle elongation. For meroamphitelic dyads, the less robust kinetochore fiber of the merotelic extends toward the pole opposite that to which its sister extends, so the merotelic shifts away from its sister during anaphase B. As predicted by Cimini's rules, if a merotelic starts anaphase in the half-spindle of its less birefringent fiber (because its nonmerotelic sister is oriented toward the pole of the half-spindle), the merotelic shifts equatorially at anaphase (also see Pidoux *et al*., 2000) into the opposite half-spindle, still away from its sister. So far, no evidence, including ours, exists for merotelics disobeying Cimini's rules.

Merosyntely (Figure 3, G and H) has been postulated previously, although not observed (Salmon *et al*., 2005), to explain nondisjunction in nocodazole-recovering mitotic cells (Cimini *et al*., 1999). Our demonstration that merosyntely is indeed induced by arrest recovery is the first for either mitosis or meiosis II and establishes it as a direct cause of nondisjunction. In contrast to chromatids of syntelics, which move all the way to the centrosome, a merotelic from a merosyntelic dyad is included in a nucleus because it starts anaphase close enough to it to fuse with nonmerotelic chromosomes that move there during anaphase.

While meroamphitely and amphitely lead to proper distribution (Figure 3, A–C), and merosyntely and syntely lead to nondisjunction (Figure 3, G–I), balanced merotelics, which remain near the equator (Figure 3, D–F), may elicit different outcomes depending on cell type. In crane fly sper-

matocytes, equatorial laggards usually cause cleavage furrow regression. Abortive cytokinesis II produces a meiotic product with twice its normal chromosome complement. In mitosis, cytokinesis failure can cause subsequent divisions to be multipolar, leading to aneuploidy (Shi and King, 2005). Similarly, laggard-induced meiosis I cytokinesis failure was shown previously to lead to a tripolar meiosis II spindle and to a spermatid containing chromosomes from one of those poles (Janicke and LaFountain, 1982). In mitotic cells where cytokinesis succeeds despite equatorial laggards, indirect nondisjunction could occur if a balanced merotelic from a dyad oriented as in Figure 3, E or F, is included in the same daughter cell as its sister, forms a micronucleus, then, during the next division, incorporates into a daughter nucleus, making it (n + 1) (Rizzoni *et al*., 1989). Alternatively, balanced merotely might lead to aneuploidy through laggard disintegration or micronucleus loss (Sugawara and Mikamo, 1980; Ford *et al*., 1988), neither of which was observed here.

Coinduction of bipolar and monopolar malorientations may be common. If so, that might help explain why coinduction of anaphase lag and nondisjunction has been reported in diverse systems (Sugawara and Mikamo, 1980; Elhajouji *et al*., 1997; Parry *et al*., 2002; Salmon *et al*., 2005; Sun *et al*., 2005). Using our scoring criteria, after 24-h arrests, the ratio of percentage of cells with anaphase lag (of all anaphase cells) at 60 min of recovery to percentage of cells with nondisjunction (of successfully cleaving cells) at 90 min of recovery was 40:1; it was 20:1 after 48-h arrests and 9:1 after 72-h arrests (Table 1). Thus, syntely and merosyntely were induced less efficiently than other malorientations, but lengthening cold exposure increased the proportion of malorientations that were syntelic or merosyntelic.

With longer arrests, metaphase II dyads in cold arrest-recovering spermatocytes more frequently displayed off-equator metaphase dyad positions, which resulted from bipolar or monopolar malorientations. Human oocytes naturally arrest in meiosis I until ovulation and in meiosis II until fertilization and have unusually high frequencies of nondisjunction. Studies on human oocytes have shown that metaphase II dyad misalignment correlates with age-dependent increased nondisjunction (Battaglia *et al*., 1996, Volarcik *et al*., 1998; Hodges *et al*., 2002; Page and Hawley, 2003). Perhaps, as in cold recovery, off-equator metaphase II dyads in oocytes resuming meiosis after natural arrests have bipolar or monopolar malorientations. If so, those that are monopolar or nearly monopolar could cause nondisjunction, as has been demonstrated in spermatocytes by the present study.

How malorientation is induced by arrest recovery remains to be resolved, as does the relationship between induction of bipolar versus monopolar malorientations. Further investigation should elucidate not only errors leading to nondisjunction but also mechanisms (Lampson *et al*., 2004; Biggins, 2004) by which chromosomes achieve the proper orientation that ensures equidistribution.

ACKNOWLEDGMENTS

We thank Alan Siegel and Grant Harris for technical assistance and Jim Stamos for assisting with illustrations. This study was supported by National Science Foundation grant MCB-0235934 (to J.L.) and grants GM 49210 from the National Institute of General Medical Sciences and EB002045 from the National Institutes of Biomedical Imaging and Bioengineering (to R.O.).

REFERENCES

Angell, R. (1997). First-meiotic division nondisjunction in human oocytes. Am. J. Hum. Genet. *61*, 23–32.

Antonio, C., Ferby, I., Wilhelm, H., Jones, M. Karsenti, E. Nebreda, A. R., and Vernos, I. (2000). Xkid, a chromokinesin required for chromosome alignment on the metaphase plate. Cell *102*, 425–435.

Battaglia, D. G., Goodwin, P., and Klein, N. A. (1996). Influence of maternal age on meiotic spindles in oocytes from naturally cycling women. Hum. Reprod. *11*, 2217–2222.

Begg, D. A., and Ellis, G. W. (1979). Micromanipulation studies of chromosome movement. 2. Birefringent chromosomal fibers and the mechanical attachment of chromosomes to the spindle. J. Cell Biol. *82*, 542–554.

Bickel, S. E., Moore, D. P., Lai, C., and Orr-Weaver, T. L. (1998). Genetic interactions between meiS332 and ord in the control of sister-chromatid cohesion. Genetics *150*, 1467–1476.

Biggins, S. (2004). Correcting SYNful attachments. Nat. Cell Biol. *6*, 181–183.

Cimini, D., Antoccia, A., Tanzarella, C., and Degrassi, F. (1997). Topoisomerase II inhibition I mitosis produces numerical and structural chromosomal aberrations I human fibroblasts. Cytogenet. Cell Genet. *76*, 61–67.

Cimini, D., Cameron, L. A., and Salmon, E. D. (2004). Anaphase spindle mechanics prevent mis-segregation of merotelically oriented chromosomes. Curr. Biol. *14*, 2149–2155.

Cimini, D., and Degrassi, F. (2005). Aneuploidy: a matter of bad connections. Trends Cell Biol. *15*, 442–451.

Cimini, D., Fioravanti, D., Salmon, E. D., and Degrassi, F. (2002). Merotelic kinetochore orientation versus chromosome mono-orientation in the origin of lagging chromsomes in human primary cells. J. Cell Sci. *115*, 507–515.

Cimini, D., Howell, B., Maddox, P., Khodjakov, A. Degrassi, F., and Salmon, E. D. (2001). Merotelic kinetochore orientation is a major mechanism of aneuploidy in mitotic ammalian tissue cells. J. Cell Biol. *153*, 517–527.

Cimini, D., Moree, B., Canman, J. C., and Salmon, E. D. (2003). Merotelic kinetochore orientation occurs frequently during early mitosis in mammalian tissue cells and error correction is achieved by two different mechanisms. J. Cell Sci. *116*, 4213–4225.

Cimini, D., Tanzarella, C., and Degrassi, F. (1999). Differences in mal-segregation rate obtained by scoring ana-telophase or binucleate cells. Mutagenesis *14*, 563–568.

Elhajouji, A., Tibaldi, F., and Kirsch-Volders, M. (1997). Indication for thresholds of chromosome non-disjunction versus chromosome lagging induced by spindle inhibitors in vitro in human lymphocytes. Mutagenesis *12*, 133–140.

Falck, G. C., Catalán, J., and Norppa, H. (2002). Nature of anaphase laggards and micronuclei in female cytokinesis-blocked lymphocytes. Mutagenesis *17*, 111–117.

Ford, J. H., Schultz, C. J., and Correll, A. T. (1988). Chromosome elimination in micronuclei: a common cause of hypoploidy. Am. J. Hum. Genet. *43*, 733–740.

Forer, A., and Pickett-Heaps, J. D. (1998). Checkpoint control in crane-fly spermatocytes: unattached chromosomes induced by cytochalasin D or latrunculin do not prevent or delay the start of anaphase. Protoplasma *203*, 100–111.

Funabiki, H., and Murray, A. W. (2000). The *Xenopus* chromokinesinXkid is essential for metaphase chromosome alignment and must be degraded to allow anaphase chromosome movement. Cell *102*, 411–424.

Gassmann, R., Carvalho, A., Henzing, A. J., Ruchaud, S., Hudson, D. F., Honda, R., Nigg, E. A., Gerloff, D. L., and Earnshaw, W. C. (2004). Borealin: a novel chromosomal passenger required for stability of the bipolar meiotic spindle. J. Cell Biol. *166*, 179–191.

Hassold, T., and Hunt, P. (2001). To err (meiotically) is human: the genesis of human aneuploidy. Nat. Rev. Genet. *2*, 280–291.

Hawley, R. S., Frazier, J., and Rasooly, R. (1994). Separation anxiety: the biology of non-disjunction in flies and people. Hum. Mol. Genet. *3*, 1521–1528.

Henderson, S. A., Nicklas, R. B., and Koch, C. A. (1970). Temperature-induced orientation instability during meiosis: an experimental analysis. J. Cell Sci. *6*, 323–350.

Hildreth, P. D., and Ulrichs, P. C. (1969). A temperature effect on nondisjunction of the X chromosomes among eggs from aged *Drosophila* females. Genetica *40*, 191–197.

Hodges, C. A., Ilagen, A., Jennings, D., Keri, R., Nilson, J., and Hunt, P. A. (2002). Experimental evidence that changes in oocyte growth influence meiotic chromosome segregation. Hum. Reprod. *17*, 1171–1180.

Janicke, M. and LaFountain, J. R., Jr. (1982). Chromosome segregation in crane-fly spermatocyts: cold treatment and cold recovery induce anaphase lag. Chromosoma *85*, 619–631.

Janicke, M. A., and LaFountain, R., Jr. (1984). Malorientation in half-bivalents at anaphase: analysis of autosomal laggards in untreated, cold-treated, and cold recovering crane-fly spermatocytes. J. Cell Biol. *98*, 859–869.

Janicke, M. A., and LaFountain, R., Jr. (1986). Bivalent orientation and behavior in crane-fly spermatocytes recovering from cold exposure. Cell Motil. Cytoskeleton *6*, 492–501.

Kapoor, T. M., Lampson, M. A., Hergert, P., Cameron, L., Cimini, D., Salmon, E. D., McEwen, B., and Khodjakov, A. (2006). Chromosomes can congress to the metaphase plate before biorientation. Science *311*, 388–391.

Karp, L. E., and Smith, W. D. (1975). Experimental production of aneuploidy in mouse oocytes. Gynecol. Investig. *6*, 337–341.

Kato, H., and Yosida, T. H. (1970). Nondisjunction of chromosomes in a synchronized cell population initiated by reversal of colcemid inhibition. Exp. Cell Res. *60*, 459–464.

Khodjakov, A., Cole, R. W., McEwen, B. R., Buttle, K. F., and Rieder, C. L. (1997). Chromosome fragments possessing only one kinetochore can congress to the spindle equator. J. Cell Biol. *136*, 229–240.

Kline-Smith, A., Khoakov, A., Herget, P., and Walczak, C. E. (2004). Depletion of centromeric MCAK leads to chromosome congression and segregation defects due to improper kinetochore attachments. Mol. Biol. Cell *15*, 1146–1159.

Koehler, K. E., Boulton, C. L., Collings, H. E., French, R. L., Herman, K. C., Lacefield, S. M., Madden, L. D., Schuetz, C. D., and Hawley, R. S. (1996). Spontaneous X chromosome MI and MII nondisjunction events in *Drosophila melanogaster* oocytes have different recombinational histories. Nat. Genet. *14*, 406–414.

Kops, G.J.P.L., Weaver, A. A., and Cleveland, D. W. (2005). On the road to cancer: aneuploidy and the mitotic checkpoint. Nat. Rev. Cancer *5*, 773–785.

Ladrach, K. S., and LaFountain, J. R., Jr. (1986). Malorientation and abnormal segregation of chromosomes during recovery from colcemid and nocodazole. Cell Motil. Cyotskeleton *6*, 419–427.

LaFountain, J. R., Jr. (1985). Chromosome segregation and spindle structure in crane fly spermatocytes following Colcemid treatment. Chromosoma *91*, 329–336.

LaFountain, J. R., Jr., Cole, R. W., and Rieder, C. L. (2002). Polar ejection forces are operative in crane-fly spermatocytes, but their action is limited to the spindle periphery. Cell Motil. Cytoskeleton *51*, 16–26.

LaFountain, J. R., Jr., and Oldenbourg, R. (2004). Maloriented bivalents have metaphase positions at the spindle equator with more kinetochore microtubules to one pole than to the other. Mol. Biol. Cell *15*, 5346–5355.

Lamb, N. E., and Hassold, T. J. (2004). Nondisjunction—a view from ringside. N. Engl. J. Med. *351*, 1931–1934.

Lamb, N. E. *et al*. (1996). Susceptible chiasmate configurations of chromosome 21 predispose to nondisjunction in both maternal meiosis I and meiosis II. Nat. Genet. *14*, 400–405.

Lampson, M. A., Renduchitala, K., Khodjakov, A., and Kapoor, T. M. (2004). Correcting improper chromosome-spindle attachments during cell division. Nat. Cell Biol. *6*, 232–237.

LeMaire-Adkins, R., Radke, K., and Hunt, P. A. (1997). Lack of checkpoint control at the metaphase/anaphase transition: a mechanism of meiotic nondisjunction in mammalian females. J. Cell Biol., *139*, 1611–1619.

Maiato, H., DeLuca, J., Salmon, E. D., and Earnshaw, W. C. (2004). The dynamic kinetochore-microtubule interface. J. Cell Sci. *117*, 5461–5477.

McEwen, B. F., Heagle, A. B., Cassels, G. O., Buttle, K. F., and Rieder, C. L. (1997). Kinetochore fiber maturation in PtK1 cells and its implications for the mechanisms of chromosome congression and anaphase onset. J. Cell Biol. *137*, 1567–1580.

Nicklas, R. B. (1997). How cells get the right chromosomes. Science *275*, 632–637.

Nicolaidis, P., and Petersen, M. B. (1998). Origin and mechanisms of nondisjunction in human autosomal trisomies. Hum. Reprod. *13*, 313–319.

Oldenbourg, R., Salmon, E. D., and Tran, P. T. (1998). Birefringence of single and bundled microtubules. Biophys. J. *74*, 645–654.

Orr-Weaver, T. (1996). Meiotic nondisjunction does the two-step. Nat. Genet. *14*, 374–376.

Page, S. L., and Hawley, R. S. (2003). Chromosome choreography: the meiotic ballet. Science *301*, 785–789.

Parry, E. M. *et al*. (2002). Detection and characterization of action of aneugenic chemicals. Mutagenesis *17*, 509–521.

Pidoux, A. L., Uzawa, S., Perry, P. E., Cande, W. Z., and Allshire, R. C. (2000). Live analysis of lagging chromosomes during anaphase and their effect on spindle elongation rate in fission yeast. J. Cell Sci. *113*, 4177–4191.

Pinsky, B. A., and Biggins, S. (2005). The spindle checkpoint: tension versus attachment. Trends Cell Biol. *15*, 486–493.

Rebollo, E., and Arana, P. (1998). Chromosomal factors affecting the transmission of univalents. Chromosome Res. *6*, 67–69.

Rizzoni, M., Tanzarella, C., Gustavino, B., Degrassi, F., Guarino A, and Vitagliano, E. (1989). Indirect mitotic nondisjunction in Vicia faba and Chinese hamster cells. Chromosoma *97*, 339–346.

Salmon, E. D., Cimini, D., Cameron, L. A., and DeLuca, J. G. (2005). Merotelic kinetochores in mammalian tissue cells. Phil. Trans. R. Soc. B *360*, 553–568.

Scarcello, L. A., Janicke, M. A., and LaFountain, J. R. (1986). Kinetochore microtubules in crane-fly spermatocytes: untreated, 2°C treated, and 6°C grown spindles. Cell Motil. Cytoskeleton *6*, 428–438.

Shannon, K. B., and Salmon, E. D. (2002). Chromosome dynamics: new light on aurora B kinase function. Curr. Biol. *12*, R458–R460.

Shi, Q., and King, R. W. (2005). Chromosome nondisjunction yields tetraploid rather than aneuploid cells in human cell lines Nature *437*, 1038–1042.

Skibbens, R. V., Skeen, V. P., and Salmon, E. D. (1993). Directional instability of kinetochore motility during chromosome congression and segregation in mitotic newt lung cells: a push-pull mechanism. J. Cell Biol. *122*, 859–875.

Sugawara, S., and Mikamo, K. (1980). An experimental approach to the analysis of mechanisms of meiotic nondisjunction and anaphase lagging in primary oocytes. Cytogenet. Cell Genet. *28*, 251–264.

Sun, F., Betzendahl, I., Pacchierotti, F., Randaldi, R., Smitz, J., Cortvrindt, R., and Eichenlaub-Ritter, U. (2005). Aneuploidy in mouse metaphase II oocytes exposed in vivo and in vitro in preantral follicle culture to nocodazole. Mutagenesis *10*, 65–75.

Tanaka, T. (2002). Bi-orienting chromosomes on the mitotic spindle. Curr. Opin. Cell Biol. *14*, 365–371.

Tokunaga, C. (1970). Aspects of low-temperature-induced meiotic nondisjunction in *Drosophila* females. Genetics *66*, 653–661.

Volarcik, K., Sheean, L., Goldfarb, J., Woods, L., Abdul-Karim, F. W., and Hunt, P. (1998). The meiotic competence of in-vitro matured human oocytes is influenced by donor age: evidence that folliculogenesis is compromised in the reproductively aged ovary. Hum. Reprod. *13*, 154–160.

Weaver, B.A.A., Silk, A., and Cleveland, D. (2006). Nondisjunction, aneuploidy and tetraploidy. Nature *442*, E9–E10.

Yu, H.-G., and Dawe, R. K. (2000). Functional redundancy in the maize meiotic kinetochore. J. Cell Biol. *151*, 131–141.